The Journal of Engineering

IET International Radar Conference (IRC 2018)

eISSN 2051-3305
Received on 20th February 2019
Accepted on 3rd May 2019
E-First on 19th July 2019
doi: 10.1049/joe.2019.0415
www.ietdl.org

Kalman filter aided target density function for radar imaging

Ridvan Firat Cinar[1] ✉, *Fatih Kocadag*[2], *Askin Demirkol*[1]

[1]*Sakarya University, Faculty of Engineering, Department of Electrical-Electronics, Sakarya, Turkey*

[2]*Abant Izzet Baysal University, I.T. Centre, Bolu, Turkey*

✉ *E-mail: ridvancinar@sakarya.edu.tr*

Abstract: This study proposes a new algorithm for air target radar imaging by taking the geometrical and processing advantages of array antenna systems. The backscattered signal is processed with a new technique to benefit the facilities of angular scanning. In order to virtually increase the number of the radar elements of the array system, a powerful optimal estimator is employed, namely Kalman filter.

1 Introduction

As an imaging idea, the usage of radio waves is one of the most sophisticated signal processing challenges. Radars are being used for detection and tracking since the Second World War. By dint of radar techniques advancement, the reach of higher bandwidths enabled the radars to have an ability of imaging.

Radar imaging techniques consider the radar image as a mapping of the scatterer densities of the target. This property makes the use of density distribution functions useful. Like an illuminated object with visible light, the consideration of the distribution function and the denser reflectors parts give more powerful backscatter and display higher peaks on radar image.

In this paper, the previous approaches and the proposed method are explained with details. The schematic representations, formulations, and simulation are achieved. The obtained results and conclusion are given [1–3].

The rest of the paper is organised as following. In Section 2, an overview of radar imaging approaches is given. The Kalman estimation and use of Kalman in array imaging are explained in Sections 3 and 4, respectively. Section 5 is focused on the implementation and results part. Finally, the conclusion is given in Section 6.

2 Radar imaging approaches

Radar imaging techniques are well studied and matured topics in the radar literature such as [3–10]. The method that is considered in this chapter represents an active sensor array imaging with variables R and β, where R is range and the $\beta = \cos(\theta)$ (i.e. cosine of the scanning angle θ). The defined function $G(R,\ \beta)$ [11] represents the intensity of the signal echoed from the point at R range and β as a function of the scanning angle θ. Imaging scenario can be seen in Fig. 1.

For a $p(t)$ signal, modulated sent signal is

$$s_m(t) = p(t)s_c(t) \tag{1}$$

Thus, the echoed signal from a $G(R,\ \beta)$ point of target scene becomes;

$$s_r(x, t) = s_m(t - \beta \mathrm{x}/c - 2R/c)g(\beta, R) \tag{2}$$

If the backscatter considered for entire imaging plane,

$$\left. S_r(x, t) = \int_{-1}^{1}\int_{0}^{R_1} \begin{matrix} p(t - \beta \mathrm{x}/c - 2R/c) \\ \times\, \mathrm{e}^{-\mathrm{j}\omega_c(\beta \mathrm{x}/c + 2R/c)}\mathrm{e}^{\mathrm{j}\omega_c t}g(\beta, R)\mathrm{d}R\mathrm{d}\beta \end{matrix} \right\} \tag{3}$$

by considering entire array, backscatter collection becomes [11–14];

$$\left. \begin{matrix} s_r(x, t) = \displaystyle\sum_{k=-\infty}^{\infty} A_k \mathrm{e}^{j(\omega_c + k\omega_0)t} \times \\ \displaystyle\int_{-1}^{1}\int_{0}^{R_1} \mathrm{e}^{-j(\omega_c + k\omega_0)(\beta \mathrm{x}/c + 2R/c)}g(\beta, R)\mathrm{d}R\mathrm{d}\beta \end{matrix} \right\} \tag{4}$$

In the next step of the algorithm, the sent signal is extracted from the backscatters by making demodulation with $s_d(t)$, to obtain information of target.

$$s_d(t) = \mathrm{e}^{-j(\omega_c + k\omega_0)t}/A_k \tag{5}$$

$$\left. S_k(x) = \int_{-\infty}^{\infty}\int_{-\infty}^{\infty} \begin{matrix} \mathrm{e}^{-j(\omega_c + k\omega_0)\beta \mathrm{x}/c}\mathrm{e}^{-j(\omega_c + k\omega_0)2R/c} \\ \times\, g(\beta, R)\mathrm{d}R\mathrm{d}\beta \end{matrix} \right\} \tag{6}$$

By taking a_k as

$$\alpha_k = (\omega_c + \mathrm{k}\omega_0)\frac{1}{c} \tag{7}$$

then, the equation becomes;

$$S_k(x) = \int_{-\infty}^{\infty}\int_{-\infty}^{\infty} g(\beta, R)\mathrm{e}^{-j(x\beta + 2R)\alpha_k}\mathrm{d}R\mathrm{d}\beta \tag{8}$$

For the mapping of $G(R,\ \beta)$ target density function, the PSD-autocorrelation function relation that is provided by ambiguity function is used [13]. Therefore, the result becomes;

$$S(\omega) = \int_{-\infty}^{\infty} A(t, \omega)\mathrm{e}^{j(\omega/2)t}\mathrm{d}t \tag{9}$$

$$G(R, \beta) = \int_{-\infty}^{\infty} s_m\left(t - \frac{\tau_R}{2}\right)\overline{s_n}\left(t + \frac{\tau_R}{2}\right)\mathrm{e}^{\mathrm{j}\beta t}\mathrm{d}t \tag{10}$$

for $\tau = r/2c$.

where $A(t,\ \omega)$ is the notation of ambiguity function that includes other operations and properties of this algorithm [11–13].

An alternative reconstruction method is represented in [14], that is successful at obtaining the density functions $G(R,\ \beta)$, by employing the modified Radon transform–Fourier slice theorem that detailed below, in (11) (Fig. 2).

$$
\left.\begin{aligned}
S_k(x,1) &= \int_{-\infty}^{\infty}\int_{-\infty}^{\infty} g(R,\beta)\mathrm{e}^{-j(x\beta+2R)\alpha_k}\mathrm{d}\beta\mathrm{d}R \\
&= \int_{-\infty}^{\infty} g(R,\beta)\mathrm{e}^{-j2R}\mathrm{d}R\int_{-\infty}^{\infty}\mathrm{e}^{-\mathrm{j}x\beta}\mathrm{d}\beta \\
&= \int_{-\infty}^{\infty} g(\beta)\mathrm{e}^{-\mathrm{j}x\beta}\mathrm{d}\beta \\
&= G(x)
\end{aligned}\right\} \tag{11}
$$

3 Kalman estimation

Kalman filter is a recursive mathematical method that quickly computes the optimal estimation from a set of stochastic measurements. The ability of estimation of the current, previous or next state of the system even under high noise level, makes this filter useful and powerful for various application fields. Kalman filter continuously finds out the change of state variables with measurements, while it minimises the mean square error [15, 16] (Fig. 3).

Kalman filter's main purpose is to estimate the state $x \in \mathfrak{R}^n$ as shown in (12),

$$\hat{x}_k^- = A\hat{x}_{k-1} + \mathrm{B}u_{k-1} + w_{k-1} \tag{12}$$

with a measurement $z \in \mathfrak{R}^m$,

$$z_k = \mathrm{H}x_k + v_k \tag{13}$$

where A is the state transition model, B is the control input model and w_k and v_k are the representations of process and measurement noise, respectively.

For discrete time applications, Kalman filter updates time and measurement coherently to make prediction of actual estimate.

Time update (prediction):

Initial estimates for $\hat{x}_{k-1}$ and P_{k-1}.

(i) Project the state ahead

$$\hat{x}_k^- = A\hat{x}_{k-1} + \mathrm{B}u_{k-1} \tag{14}$$

(ii) Project the error covariance ahead

$$P_k^- = \mathrm{A}P_{k-1}A^{\mathrm{T}} + Q \tag{15}$$

The time update equations can also be thought of as predictor equations, while the measurement update equations can be thought of as corrector equations [15–18].

Measurement update (correction):

(i) Compute the Kalman gain

$$K_k = P_k^- H^{\mathrm{T}}(\mathrm{H}P_k^- H^{\mathrm{T}} + R)^{-1} \tag{16}$$

(ii) Update estimate with measurement z_k

$$\hat{x}_k = \hat{x}_k^- + K_k(z_k - \mathrm{H}\hat{x}_k^-) \tag{17}$$

(iii) Update the covariance of error

$$Pk = (I - K_k H)P_k^- \tag{18}$$

4 Kalman-aided array imaging

For the given method in Sections 2 and 3, array processing provides geometric and processual benefits like imaging under a short observation time and observation angle to display more scatterer points from diverse angles [19].

However, in this method, construction of an array with large quantities of individual elements may cause high cost in terms of implementation. This work suggests employing the Kalman method to efficiently decrease the number of elements in the array and estimate missing target density functions caused by decrement, with high stability.

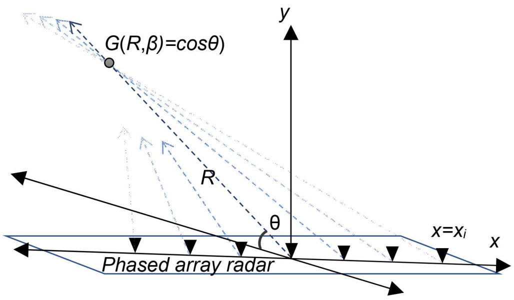

Fig. 1 *Imaging with phased array system and Target Density Functions (TDF)*

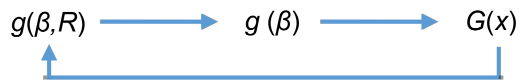

Fig. 2 *Fourier slice theorem for g (R, β)*

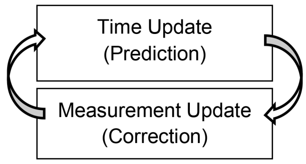

Fig. 3 *Kalman filter cycle*

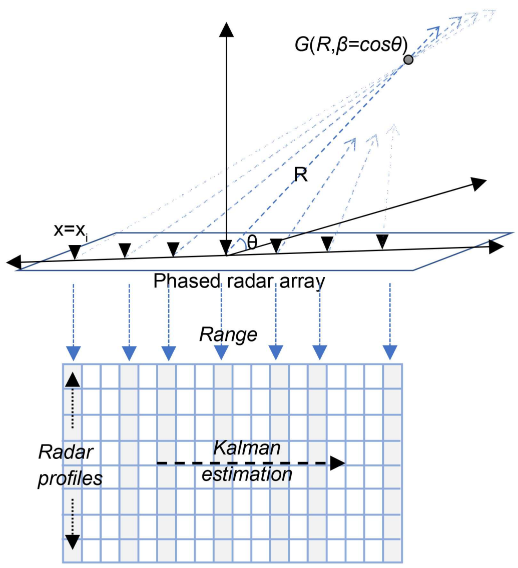

Fig. 4 *Obtaining data and imaging scenario*

As can be seen in the scenario in Fig. 4, Kalman estimation is applied along the $\beta = \cos\theta$ direction for $\theta\mathrm{min} < \theta i < \theta\mathrm{max}$ to build virtual radar profiles and indirectly increases the angular properties such as resolution.

5 Implementation and results

Fig. 5 shows the density distribution of the scatter points that is reconstructed by the Fourier Slice Theorem based on the method referenced in [14].

Figs. 6–8 show the results of the reconstruction of target density functions using phased array active sensors that has different numbers of individual elements, respectively, 32 elements, 21 elements, and 16 elements increased by using Kalman estimation to 64 elements.

The theoretical target of the simulation system is a fighter aircraft with multiple reflective points that clearly display the outer edges and dense scatter points of the target such as nose and

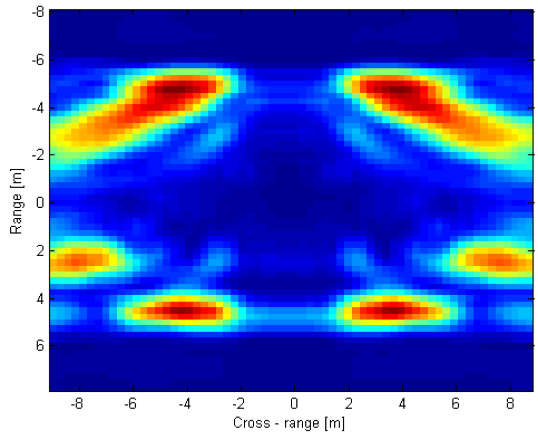

Fig. 5 *density distribution of the scatter points that is reconstructed by the theorem in [14]*

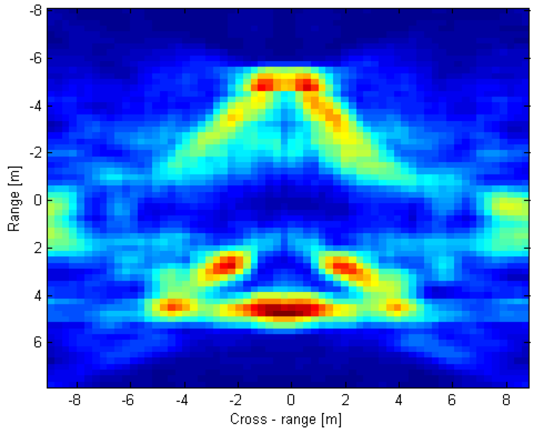

Fig. 6 *density distribution of the scatter points that is reconstructed with array increased from 32 to 64*

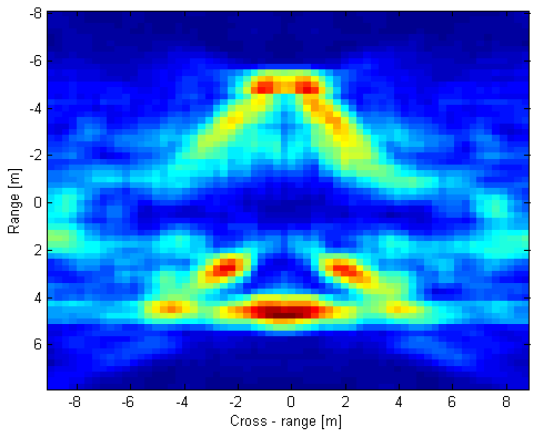

Fig. 7 *Density distribution of the scatter points that is reconstructed with array increased from 21 to 64*

wingtips. The total scanning angle of the system is 54 degrees with resolution $\delta r = 0.24$ m and $\delta x = 0.28$.

6 Conclusion and future work

This paper presented a new radar imaging approach with Kalman estimation. The proposed method decreases imaging implementation costs. The results of simulation show that the

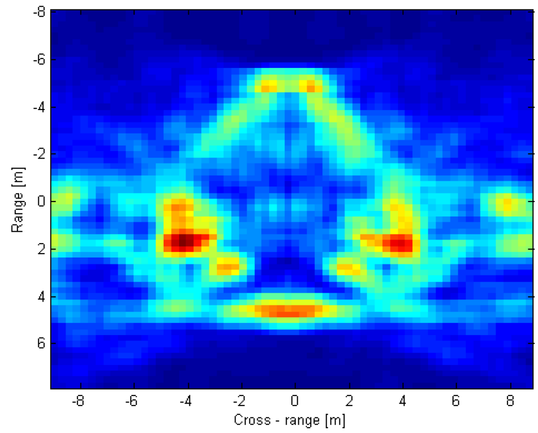

Fig. 8 *Density distribution of the scatter points that is reconstructed with array increased from 16 to 64*

offered imaging technic is able to give result under different (virtually increased) array formation. The use of Kalman estimation demonstrates the powerfulness of this approach. The results obtained show that the virtual increasing of the array numbers with Kalman estimation gives more suitable results when one increases the array elements from 32 to 64 and 21 to 64. The results can be seen in Figs. 5–7, respectively, except in Fig. 8 where the interpolation of the Kalman estimation shows some weakness. Multi-target imaging and refocusing with Kalman filter can be considered in future works.

7 References

[1] Skolnik, M.I.: '*Introduction to radar systems*' (McGraw-Hill, NY, 1980, 2nd edn.)

[2] Woodward, P.M.: 'Probability and information theory with applications to radar', 1957

[3] Chen, V.C., Ling, H.: '*Time-frequency transforms for radar imaging and signal analysis*' (Artech House, Norwood, MA, USA, 2002)

[4] Chen, V.C., Qian, S.: 'Time frequency transform vs. Fourier transform for radar imaging'. Time - Frequency and Time - Scale Analysis, 1996., Proc. of the IEEE-SP Int. Symp. on, Paris, France, 18–21 June 1996, pp. 389–392

[5] Fornaro, G., Pascazio, V.: '*Academic press library in signal processing*' Communications and Radar Signal Processing. Academic Press Library in Signal Processing, (Elsevier, New York, NY, USA, 2014), Vol. **2**, pp. 1043–1117

[6] Birk, R., Camus, W., Valenti, E., *et al.*: 'Synthetic aperture radar imaging systems', *IEEE Aerosp. Electron. Syst. Mag.*, 1995, **10**, (11), pp. 15–23

[7] Ozdemir, C.: '*Inverse synthetic aperture radar imaging with MATLAB algorithms*' (John Wiley & Sons, Inc., Publication, New Jersey, NJ, USA, 2012)

[8] Fowle, E.N., Kelly, E.J., Sheehan, J.A.: 'Radar system performance in a dense-target environment', *IRE Int. Conv. Rec.*, 1961, **4**, pp. 136–145

[9] Naparst, H.L.: 'Radar signal choice and processing for a dense target environment'. Ph.D. thesis, Univ. of California, Berkeley, Ann Arbor, MI, University Microfilms, Inc., 1988

[10] Naparst, H.: 'Dense target signal processing', *IEEE Trans. Inf. Theory*, 1991, **37**, (2), pp. 317–327

[11] Cinar, R.F., Demirkol, A., Demir, Z.: 'An ambiguity function aided target density function for radar imaging', *OAM-RC*, 2015, **9**, (5–6), pp. 850–854

[12] Demirkol, A.: 'Range density function for active sensor imaging', *Def. Sci. J.*, 2007, **57**, (3), pp. 305–313

[13] Levanon, N., Mozeson, E.: '*Radar signals*' (Wiley IEEE, New York, 2004)

[14] Cinar, R.F., Demirkol, A.: 'Reconstruction of a radar target density function using radon transform'. 2016 CIE Int. Conf. on Radar (RADAR), IEEE, 2016

[15] Brown, R.G., Hwang, P.Y.C.: '*Introduction to random signals and applied Kalman filtering*' (John Wiley & Sons, Inc., New York, NY, USA, 1992, 2nd edn.)

[16] Mohinder, S.G., Andrews, A.P.: '*Kalman filtering: theory and practice with MATLAB*' (Wiley-IEEE Press, New Jersey, NJ, USA, 2014, 4th edn.)

[17] Welch, G., Gray, B.: '*An Introduction to the Kalman filter*', (University of North Carolina, Chapel Hill, NC, USA, 2006), pp. 5–7

[18] Welch, G., Bishop, G.: 'An introduction to the Kalman filter', '*SIGGRAPH 2001, course 8*' 27599-23175, Los Angeles, CA, USA, 2001, pp. 19–41

[19] Wirth, W.-D.: 'Radar techniques using array antennas', *IET*, 2001, **10**, pp. 51–57